Simulation and development of a coded source neutron imaging system

Philip Bingham and Hector Santos-Villalobos

Imaging, Signals and Machine Learning Group, Oak Ridge National Laboratory (ORNL), Oak Ridge TN

Abstract

Neutron radiography was first introduced in the 1930s and has seen use in non-destructive testing in aerospace, nuclear, and other industries in which there is a need to inspect for cavities or light materials within a heavy material. Neutrons provide a complimentary radiograph to x-rays that can provide a more complete picture of an object under test.

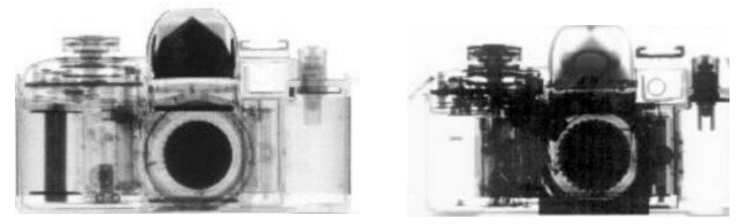

Neutron (left) and x-ray (right) radiographs of film camera (Paul Scherrer Institut, http://neutra.web.psi.ch/What/index.html)

Today's neutron radiography systems commonly provide resolutions down to the 50-100μm range using CCD cameras with a scintillation screen. Higher resolutions (10-15μm) are achieved using microchannel plate (MCP) detectors. Resolution is currently limited by the detectors as no magnification is used. The goal of this effort is to develop higher resolution neutron imaging systems through the use of coded source imaging to provide magnification without the loss in flux from a single pinhole illumination source.

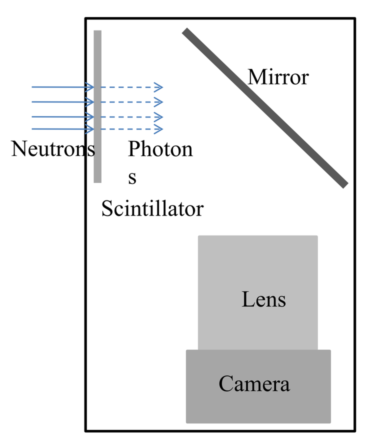

(Left) Neutron imaging detector design consisting of scintillator, mirror and CCD camera

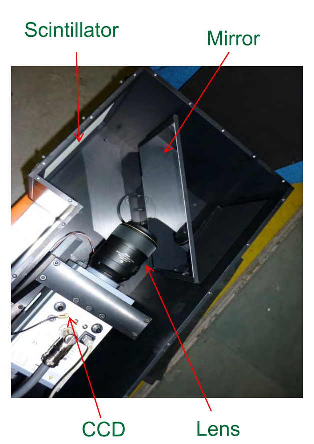

(Right) Imaging detector at the High Flux Isotope Reactor (HFIR) CG1-D Neutron Imaging Prototype Station

Introduction
Neutron Imaging

Due to the inefficiency and high cost of optical components for neutrons, imaging instruments perform direct imaging. Resolution of a direct system depends on the size of the source and distances between source, object, and detector.

Size of the neutron source (D) shows a direct relationship with resolution of the spot and distance from source to detector has an inverse relationship with resolution; therefore, L/D is used to specify the quality of neutron imaging beam lines

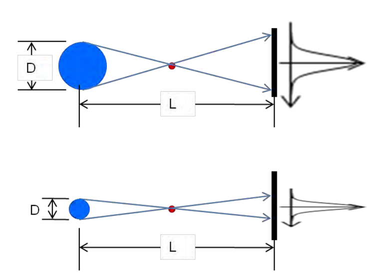

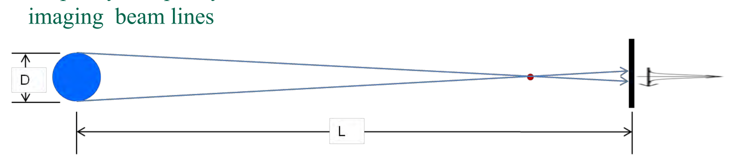

To provide the highest flux possible with reasonable exposure times, objects are imaged as close to the detector as possible. In this no magnification system, resolution depends directly on the detector. For CCD based systems, resolution is limited by the scintillation screen. As screens reduce in thickness, resolution does improve but efficiency drops. MCP detectors are reaching physical limits in the 10-15μm. Use of magnification in the imaging system will remove the resolution limitations from the detector and place them on the source size. Reducing spot size to obtain resolutions higher than currently achievable reduces flux to a level that is not suitable for imaging.

Research supported by the U.S. Department of Energy, Basic Energy Sciences (DOE-BES) with a portion of the effort performed at Oak Ridge National Laboratory's High Flux Isotope Reactor which is sponsored by the Scientific User Facilities Division of U.S. DOE-BES.

Introduction
Coded Source Imaging

Coded aperture imaging (CAI) is a well researched method for imaging sources and has been applied in areas from astronomy to homeland security. CAI uses a coded aperture (CA) with many pinholes in a well defined pattern to image the source onto a detector. Multiple pinholes allow improved signal on the detector from the source, but results in a coded image. CAs such as uniformly redundant arrays have been designed that have a defined decode kernel to reconstruct the source and have an open aperture of 50%. Coded source imaging (CSI) places a CA between an illumination source and an object to be imaged. This allows the object to be imaged with many high resolution pinholes for magnified imaging without the loss in flux associated with a single pinhole. The resulting coded radiograph follows the same math as CAI allowing use of the CAs and decode kernels already developed for CAI.

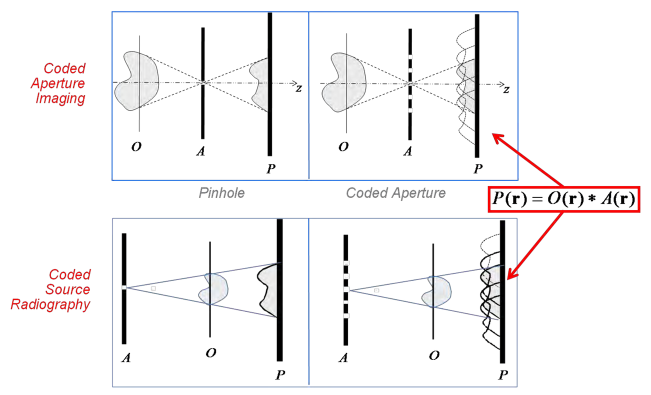

Comparison of coded aperture imaging and coded source imaging

- **Image formation**

$$P(\mathbf{r}) = O(\mathbf{r}) * A(\mathbf{r})$$

- **Reconstruction**
  - **Algorithm**

$$\hat{O}(\mathbf{r}) = P(\mathbf{r}) * G(\mathbf{r})$$

$$\hat{O}(\mathbf{r}) = O(\mathbf{r}) * \left(A(\mathbf{r}) * G(\mathbf{r})\right)$$

  - **Kernel**

$$\hat{O}(\mathbf{r}) = O(\mathbf{r}) \quad iff \quad A(\mathbf{r}) * G(\mathbf{r}) = \delta(\mathbf{r})$$

$$G(\mathbf{r}) \equiv \begin{cases} 1 & if \quad A(\mathbf{r}) = 1 \\ -1 & if \quad A(\mathbf{r}) = 0 \end{cases}$$

Simulation

A series of simulations have been performed to understand performance of CSI for neutron imaging. Simulations are being performed with McStas. First simulations were performed imaging a single pinhole object. Imaging a pinhole results in an image of the aperture pattern which allowed debugging and verification of the model with theoretical calculations.

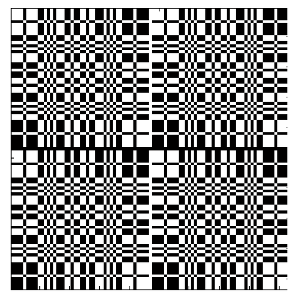

47x47 modified uniformly redundant array (MURA) pattern with 100μm pitch

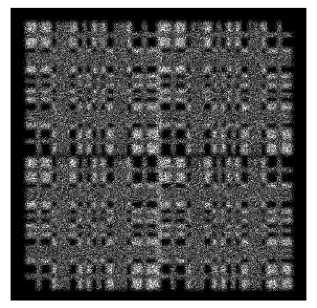

Simulated Detector image from pinhole object using 47x47 MURA

CAI provide perfect reconstruction for single point sources, so a set of simulations was performed with arrays of pinholes to evaluate performance as an object becomes more extended. In these simulations, the source is uniform and the detector resolution high enough to ignore such that performance depends on the object and reconstruction. The coded aperture is a 47x47 MURA pattern with 100μm pitch. Objects are pinhole arrays with 50μm diameter holes. Four simulations were performed with different pinhole spacing.

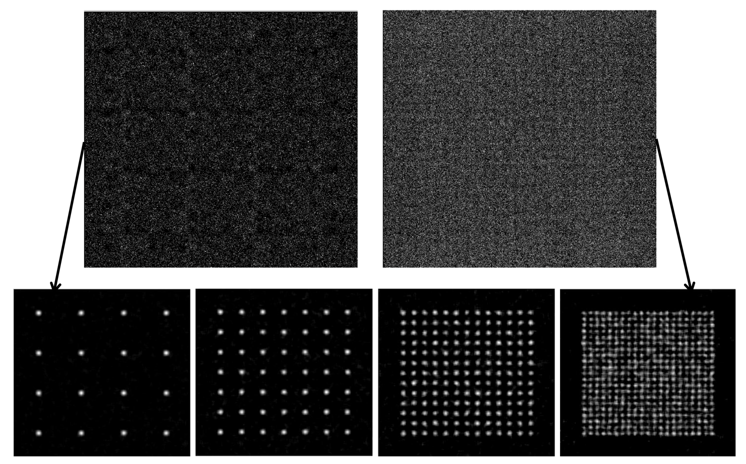

Simulation of pinhole arrays (top row) CA images of 4x4 array and 21x21 array (bottom row) reconstructed images for arrays with hole spacing of 950μm, 475μm, 237.5μm, and 142.5μm

Resolution for all 4 results is good as pinhole size of 50μm is below the resolution of the CA. For all four of these results, the number of neutrons simulated from the source is the same. As the open area for the object increases, more statistics are needed to decode the coded pattern. The low statistics and approaching the expected resolution limit of 100μm results in the noise seen in the 21 x 21 simulation result.

For quantitative measurement of resolution resulting from the CAI system, simulations of a tilted edge were performed. After reconstructing the image, a line edge function was extracted from the image and processed to provide the modulation transfer function (MTF). Simulations were performed with a 10μm and a 100μm CA mask. Using a 10% contrast level cutoff, resolution for the 10μm mask is at 50 line pairs/mm (10μm).

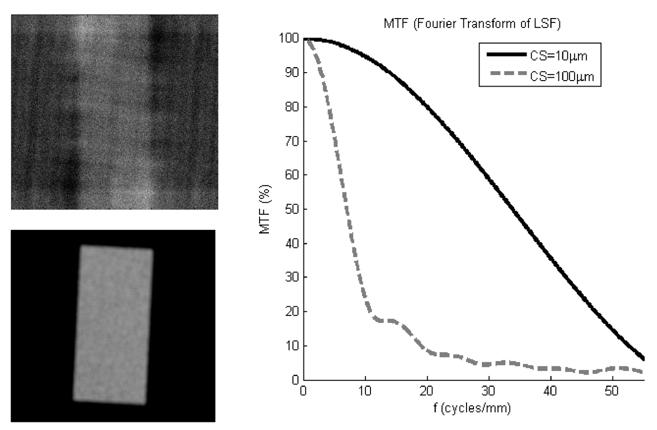

(Top left) Simulated CA image of tilted edge object, (Bottom left) image from reconstruction, and (Left) MTF calculation for 10μm and 100μm CA simulations

Development

The design of the coded aperture imaging instrument being developed is shown below. In this system, two apertures are used as an aperture/anti-aperture pair.

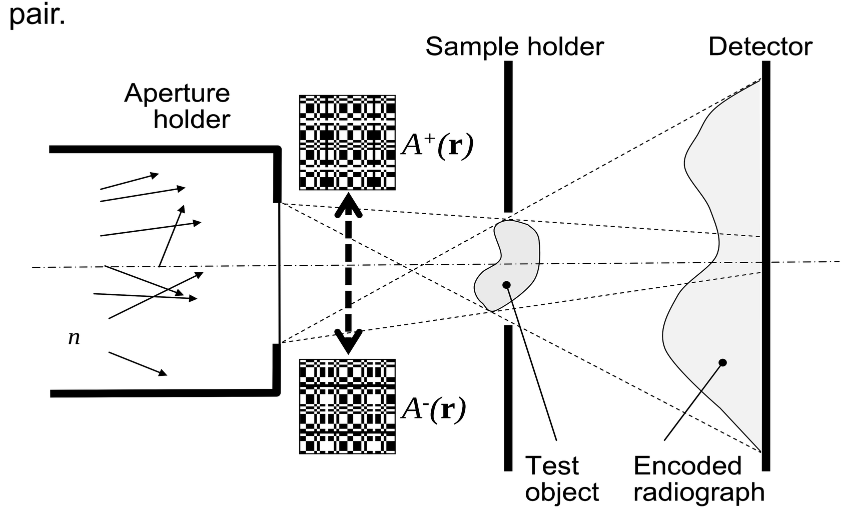

Anti-apertures are nearly the opposite pattern of the aperture with holes and filled areas swapped. From the reconstruction mathematics, the subtraction of the two images before reconstruction will remove system noise from the reconstructed image.

$$\begin{aligned} O_R(\mathbf{r}) &= [P^+(\mathbf{r}) - P^-(\mathbf{r})] * G^+(\mathbf{r}) \\ &= \left[O(\mathbf{r}) * A^+(\mathbf{r}) + n(\mathbf{r}) - \left(O(\mathbf{r}) * A^-(\mathbf{r}) + n(\mathbf{r})\right)\right] * G^+(\mathbf{r}) \\ &= O_R^+(\mathbf{r}) + O_R^-(\mathbf{r}) \end{aligned}$$

Analysis of the CAI geometry has been performed to develop equations relating system parameters of source size, divergence, and aperture size to maximum field of view for proper reconstruction. If an object extends beyond the allowed field of view, overlap from the side lobes occurs in reconstruction.

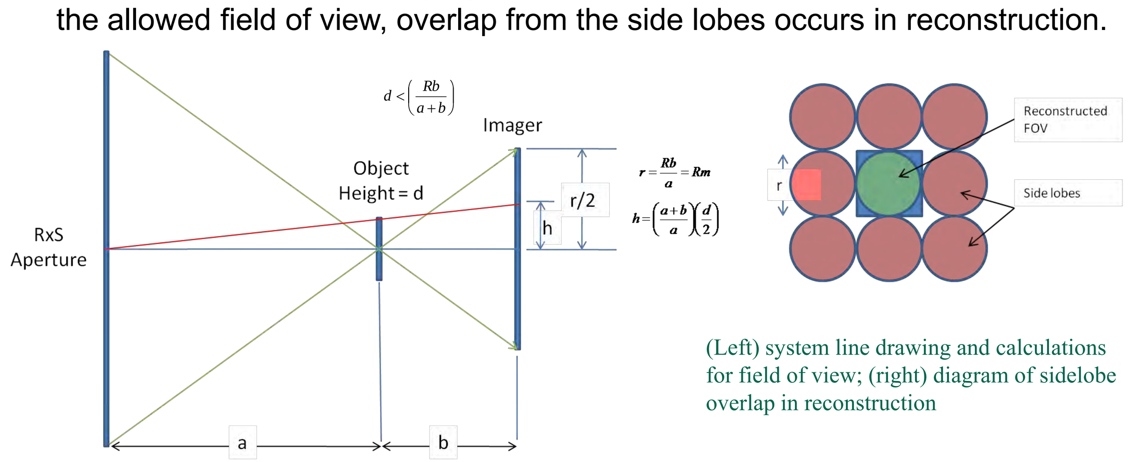

(Left) system line drawing and calculations for field of view; (right) diagram of sidelobe overlap in reconstruction

Development of a two stage system to facilitate movement of the aperture pair and the object has been completed and tested during experiments. Designs for coded apertures to be used at HFIR have been selected based on beam parameters measured in earlier tests.

A major development challenge for development is the manufacture of CA patterns with resolutions in the 1-10μm range. Investigation of manufacture methods has lead to semiconductor manufacturing capabilities. Working with CNMS at ORNL, first tests at sputtering Gd on a Si wafer were very successful at 1μm thickness.

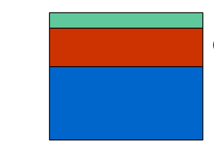

CA mask being developed on Si wafer with Gd masking material and Ti to prevent oxidization of Gd

Experimentation

With basic design and performance calculations complete for the system, an experimentation phase is underway to verify performance in an imaging system.

A 5x5 MURA pair was manufactured with no two holes touching by drilling holes in a borated Al sheet. Holes are 381μm in diameter and 0.7mm center to center spaced. This CA pair provides low resolution, but it was easy to manufacture and allows experimentation with alignment, development of reconstruction, and gives experience with the imaging beam line performance.

Aperture/anti-aperture pair manufactured by drilling 381μm holes in 1mm thick borated Al

Experiments have been performed at the CG1A and CG1D instruments at HFIR. CG1D is a white beam cold neutron imaging system. CG1A is a monochromatic beam formed using a crystal to pick off a portion of the CG1 beam.

CG1A development beam line

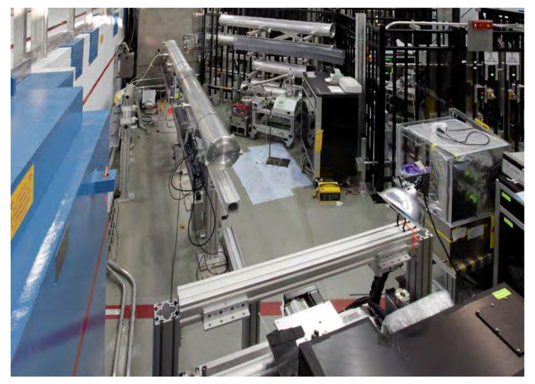

CG1D Neutron imaging prototype station

Initial experiments imaging a 1mm diameter pinhole object have been performed at both stations. Non-uniformity of illumination is a concern for both of these stations.

CG1A was set up with a magnification of 6.48. With this setup, resolution is expected to be 322μm. Images are shown with simulation results for comparison. The aperture pattern is noticeably dim on the top left and bottom right corners of the images. An image taken without the coded apertures shows the non-uniformity of the beam.

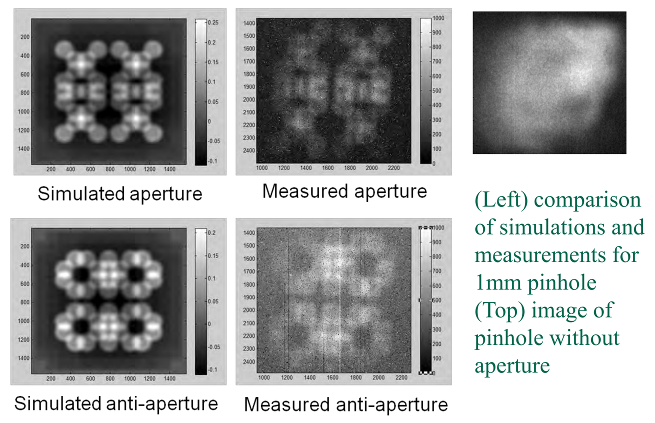

(Left) comparison of simulations and measurements for 1mm pinhole (Top) image of pinhole without aperture

Reconstruction of the pinhole is relatively unaffected by the non-uniformity as the central portion of this image is all that is required for reconstruction. The 1mm pinhole reconstruction is shown below with a line extracted across the pinhole. Based on pixel size of the detector and magnification of the system, the reconstructed hole size is 0.929mm which is well within the expected resolution.

Images were also taken of a line object. Reconstructions of extended objects are degraded significantly by the illumination uniformity and algorithm work is underway to develop methods for normalization.

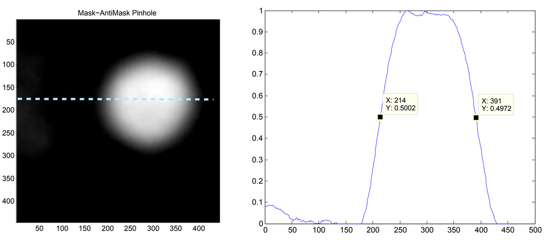

(Left) 1mm pinhole reconstruction (Right) line through center of reconstructed pinhole

Next Steps

Develop normalization methods for non-uniformity correction

Equations for image formation are being revisited to investigate approximate methods to remove non-uniform illumination. Data has recently been collected with open beams on CG1A for use in this effort.

Extension to 3-dimensional objects

Simulation and reconstruction to date has focused on two-dimensional objects. Next step is to extend to 3D objects.

High resolution aperture development

Success of sputtering 1μm of Gd on Si wafer indicates thicknesses of 10μm or more are achievable. Testing of methods for etching materials are schedule to begin this month to determine resolution and thickness limitations.

System development

High energy gammas result from neutron interactions with Gd, so shielding needs to be developed for the high resolution mask. Selection and inclusion of a perpendicular x-ray radiography system.

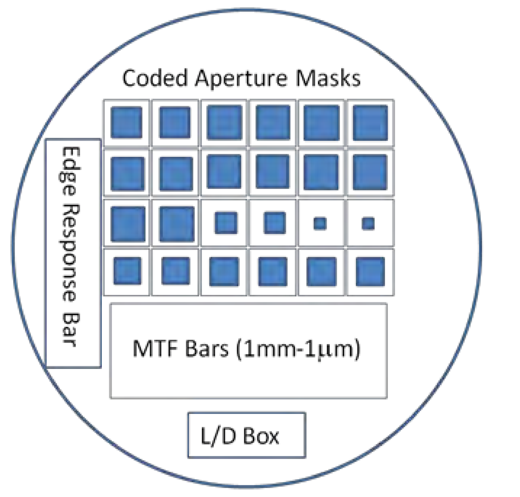

Initial plan for coded aperture wafer to include multiple aperture designs and testing features